Front. Phys. China (2007) 1: 55−62
DOI 10.1007/s11467-007-0009-4

RESEARCH ARTICLE

ZHAO Hong-kang

Shot noise in nano-electronic systems under the perturbation of ac fields

Abstract Current noise exists in circuits and electronic devices generally, and it exhibits specific features as the system reaches nanometer size. The noise in the nano-system where external ac fields are applied plays an important role, since the properties of the fields and the nano-system together govern the resulting noise. In this paper, we present the derivation of shot noise by employing the non-equilibrium Green's function technique. The more general formulas for the current correlation and noise spectral density are given. The system is composed of a central nano-system coupled to electrodes, and the obtained noise formulas are related to the Green's functions of detailed central regime and the terminals. As an example, we have performed the numerical calculation on a system with a toroidal carbon nanotube coupled to normal metal leads. The noise and Fano factor show intimate relation with the structure of the system and ac fields. The Aharonov-Bohm-like behaviors on the shot noise spectral density and Fano factor are observed to exhibit oscillation structures with period of quantum flux.

Keywords shot noise, current correlation, mesoscopic system, carbon nanotube

PACS numbers 73.40.-c, 73.63.Fg, 73.61.Wp, 73.22.-f

1 Introduction

Noise exists in electronic circuits and devices, and it is important for electronics engineers in designing new equipment. There are several types of noise in electronic systems, such as thermal noise, Nyquist-Johnson noise, $1/f$ noise, telegraphic noise, and shot noise. Usually, noise can be classified as either external noise or intrinsic noise. $1/f$ noise and telegraphic noise are external noise, since they are induced by the time-fluctuation between the interaction of system conductance and the environment. Thermal noise, Nyquist-Johnson noise and shot noise contribute to the intrinsic noise; they reflect the fluctuation of the electron occupation number during electron transport. The current tunneling through a conductor may fluctuate in time to create noise despite being under a stationary biased voltage. The noise is usually characterized by its power spectrum at frequency ω, which is defined as the Fourier transform of the current correlation function [1, 2]. For a conventional macroscopic dissipative conductor at equilibrium, the generalized Nyquist current noise spectral density [3] is given by $P(\omega) = 4G\varepsilon(\omega, T)$, where $\varepsilon(\omega, T)$ is the energy of a harmonic oscillator, and G is the conductance of the conductor. Johnson-Nyquist noise [4] is the equilibrium fluctuations due to random motion of the charge carriers. The shot noise is a non-equilibrium fluctuation that is caused by the discreteness of the charge carriers [5−7]. Yurke and Kochanski have investigated the momentum noise of barriers in the single-channel approximation by using a second quantization [8]. Beenakker and van Houten have presented a quasi-classical discussion of fluctuation with a view of ballistic transport [9]. When the size of an electronic system reaches the nanometer scale, noise becomes a very interesting problem. As the sample gets smaller, its charging energy increases and eventually becomes larger than the thermal energy. Electrons traveling through a device become correlated in the same channel and same probe, as well as in different channels and different probes. The charging and discharging electric currents therefore have strong correlation. Many specific phenomena are associated with noise, such as impedance fluctuation and Coulomb blockade. In a macroscopic system, the generalized Nyquist current noise spectral density is related to the con-

ZHAO Hong-kang (✉)
Department of Physics, Beijing Institute of Technology,
Beijing 100081, China
E-mail: zhaohonk@yahoo. com

Received October 23, 2006

ductance. But in a mesoscopic system, this relation is valid only in very special conditions. Büttiker used scattering theory to study the dynamic conductance and shot noise at low-frequency, and obtained remarkable results on these quantities by considering the first term of expansions [10, 11]. The frequency dependence of the noise spectrum has been studied by several authors [12–16].

The investigation on the deviations from the purely Poissonian shot noise in mesoscopic systems has become an increasingly interesting subject. From the investigation of shot noise, we can learn additional information on electronic structure, transport properties, and electron-electron interactions, since it is directly related to the degree of randomness in carrier transfer. Due to the Poissonian distribution in a macroscopic system, the current shows the value of shot noise by the well-known Schottky formula $S_P = 2e\langle I\rangle$. However, for a mesoscopic system, the electrons are correlated due to coherent transport, and they are governed by the Fermi distribution and the Pauli principle. This quantum behavior results in the deviation of shot noise to the Poissonian one. The suppression [17–19] and enhancement [20–22] of shot noise have been studied actively to classify the cause of the deviation of Poissonian form. Negative correlations between current pulses can lead to a complete suppression of the shot noise in quantum point contacts. Fano factor $F = S_I(\Omega)/2e\langle I\rangle$ is used to measure the suppression and enhancement of shot noise. When $F < 1$, the noise is sub-Poissonian, and when $F > 1$, it is super-Poissonian. In fact, shot noise is sensitive to the properties of a particular system. For the non-equilibrium Kondo system, the shot noise in an applied magnetic field can actually exceed the Poisson value, which can be explained by virtual processes involving the tunneling pairs of electrons with opposite spin. The singularities in the noise spectrum at $\Omega = \pm 2\ eV/\hbar$ are observed in this system [23], which is twice the conventional frequencies. For the Aharonov-Bohm mesoscopic ring threaded through an ac flux [24], the spectral density of shot noise has the singularities at $eV = n\hbar\omega$ when the "internal" frequency $eV/\hbar$ is a multiple of the external frequency ω of the applied time-dependent field. The author has investigated the thermal noise of dc Josephson current in the superconductors coupled with a quantum dot system, and the shot noise in the normal metal-quantum-dot-superconductor system.

This paper investigates the shot noise in mesoscopic systems under the perturbation of external ac fields. Generally, the system is composed of a central regime connected to multi-terminals and a gate. The external ac fields can be attributed to the microwave fields irradiating to the central regime and the terminals. The noise is induced by the current fluctuation, and the ac fields provide novel channels for the electron to tunnel. We first derive the tunneling current operator, and employ the non-equilibrium Green's function technique to derive the time-dependent current-current correlation. The noise spectral density is usually given by taking Fourier transformations. After obtaining the formula of noise, the spectral density of noise related to the carbon nanotube systems are put into consideration.

2 Formalism and derivation of noise

Generally, we consider the system composed of three parts: the two terminals and the central regime. The terminals can be made of normal metal, carbon nanotubes, and ferromagnetic materials. The central regime is written as the Hamiltonian of a quantum dot. However, it can be the sample made of toroidal carbon nanotube in our system. Here we assume that the terminal Hamiltonian is in the diagonal form, and the spin-flip effect is involved in our system for generalization. We show the system in Fig. 1.

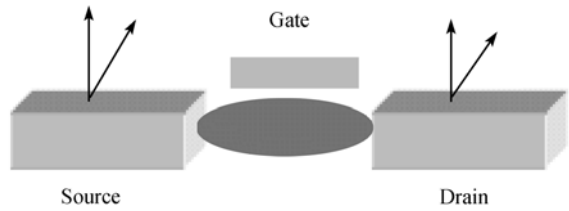

Fig. 1 The Schematic graph of the system.

The total Hamiltonian consists of the three separate parts and the interacting terms:

$$H = \sum_{\gamma k\delta\sigma} \varepsilon_{\gamma\delta,k\sigma} a^{\dagger}_{\gamma\delta,k\sigma} a_{\gamma\delta,k\sigma} + \sum_{\ell\sigma}\Big(E_{d,\ell\sigma} d^{\dagger}_{\ell\sigma} d_{\ell\sigma} + \frac{1}{2} U_{\ell} n_{\ell\sigma} n_{\ell\bar{\sigma}} \Big) + \sum_{\gamma k\delta\ell}\sum_{\sigma\sigma'}\Big[\tilde{T}^{\sigma\sigma'}_{\gamma k}(t) a^{\dagger}_{\gamma\delta,k\sigma} d_{\ell\sigma'} + \tilde{T}^{\sigma\sigma'*}_{\gamma k}(t) d^{\dagger}_{\ell\sigma'} a_{\gamma\sigma,k\sigma} \Big] \tag{1}$$

The operators $a^{\dagger}_{\gamma\delta,k\sigma}(a_{\gamma\delta,k\sigma})$ and $d^{\dagger}_{\ell\sigma}(d_{\ell\sigma})$ represent the creation (annihilation) electron operators of the terminals and central regime.

The tunneling current operator in the γth lead is derived from the continuity equation and Heisenberg equation to be

$$\hat{I}_{\gamma}(t) = \frac{ie}{\hbar}\sum_{\delta\ell k}\sum_{\sigma\sigma'}\Big[\tilde{T}^{\sigma\sigma'}_{\gamma k}(t) a^{\dagger}_{\gamma\delta,k\sigma}(t) d_{\ell\sigma'}(t) - \tilde{T}^{\sigma\sigma'*}_{\gamma k}(t) d^{\dagger}_{\ell\sigma'}(t) a_{\gamma\delta,k\sigma}(t) \Big] \tag{2}$$

The current of γth lead is given by taking the quantum average over the compound quantum state and ensemble average, i. e., $I_{\gamma}(t) = <\hat{I}_{\gamma}(t)>$. The compound quantum state is composed of the electrons of different parts and the tunneling state. The current noise is determined by the correlation terms of current fluctuation:

$$\Pi_{\gamma\gamma'}(t,t') = <\delta\hat{I}_{\gamma}(t)\delta\hat{I}_{\gamma'}(t')> + <\delta\hat{I}_{\gamma'}(t')\delta\hat{I}_{\gamma}(t)> \tag{3}$$

where $\delta\hat{I}_{\gamma}(t) = \hat{I}_{\gamma}(t) - <\hat{I}_{\gamma}(t)>$. The symbol $<\cdots>$ in the above formula denotes the quantum expectation over the

electron state, and the ensemble average over the system. Substituting the current operator Eq. (2) into Eq. (3), we encounter the expectation value of the current operator, and the four operator terms exhibit in the formula. We employ Wick's theorem in our system, and the ensemble average of the products of four electron operators are expressed by the ensemble average of the products of two electrons with one creation and one annihilation operators. We therefore obtain the following correlation function of tunneling currents:

$$\begin{aligned}\Pi_{\gamma\gamma'}(t,t') = -2e^2\mathrm{Re}\sum_{\delta\delta' kk'}\sum_{\ell\ell_1}\sum_{\sigma\sigma'}\sum_{\sigma_1\sigma_1'}\Big\{&\tilde{T}^{\sigma\sigma'}_{\gamma k}(t)\\ &\times\tilde{T}^{\sigma_1\sigma_1'}_{\gamma' k'}(t')<a^{\dagger}_{\gamma\delta,k\sigma}(t)d_{\ell_1\sigma_1'}(t')><d_{\ell\sigma'}(t)a^{\dagger}_{\gamma'\delta',k'\sigma_1}(t')>\\ &-\tilde{T}^{\sigma\sigma'}_{\gamma k}(t)\tilde{T}^{\sigma_1\sigma_1'*}_{\gamma' k'}(t')<a^{\dagger}_{\gamma\delta,k\sigma}(t)a_{\gamma'\delta',k'\sigma_1}(t')>\\ &\times<d_{\ell\sigma'}(t)d^{\dagger}_{\ell_1\sigma_1'}(t')>-\tilde{T}^{\sigma\sigma'*}_{\gamma k}(t)\tilde{T}^{\sigma_1\sigma_1'}_{\gamma' k'}(t')\\ &\times<d^{\dagger}_{\ell\sigma'}(t)d_{\ell_1\sigma_1'}(t')><a_{\gamma\delta,k\sigma}(t)a^{\dagger}_{\gamma'\delta',k'\sigma_1}(t')>\\ &+\tilde{T}^{\sigma\sigma'*}_{\gamma k}(t)\tilde{T}^{\sigma_1\sigma_1'*}_{\gamma' k'}(t')<d^{\dagger}_{\ell\sigma'}(t)a_{\gamma'\delta',k'\sigma_1}(t')>\\ &\times<a_{\gamma\delta,k\sigma}(t)d^{\dagger}_{\ell_1\sigma_1'}(t')>\Big\}\end{aligned} \tag{4}$$

The above current correlations can be expressed by the non-equilibrium Green's functions, and it is convenient to derive the shot noise by employing these functions. Here we define the Keldysh Green's functions of the terminals by

$$G^{<}_{\gamma\delta'k'\sigma_1,\gamma\delta k\sigma}(t',t) = \frac{\mathrm{i}}{\hbar}<a^{\dagger}_{\gamma\delta,k\sigma}(t)a_{\gamma\delta',k'\sigma_1}(t')> \tag{5}$$

$$G^{>}_{\gamma\delta k\sigma,\gamma\delta'k'\sigma_1}(t,t') = -\frac{\mathrm{i}}{\hbar}<a_{\gamma\delta,k\sigma}(t)a^{\dagger}_{\gamma\delta',k'\sigma_1}(t')> \tag{6}$$

The Keldysh Green's functions of electrons in the central regime are defined by

$$G^{<}_{\ell_1\sigma_1,\ell\sigma}(t',t) = \frac{\mathrm{i}}{\hbar}<d^{\dagger}_{\ell\sigma}(t)d_{\ell_1\sigma_1}(t')> \tag{7}$$

$$G^{>}_{\ell\sigma,\ell_1\sigma_1}(t,t') = -\frac{\mathrm{i}}{\hbar}<d_{\ell\sigma}(t)d^{\dagger}_{\ell_1\sigma_1}(t')> \tag{8}$$

There are four Keldysh Green's functions associated with the correlation of electrons between the central regime and the terminals. The first pair of these kinds of Keldysh Green's functions are defined as:

$$G^{<}_{\ell\sigma',\gamma\delta k\sigma}(t',t) = \frac{\mathrm{i}}{\hbar}<a^{\dagger}_{\gamma\delta,k\sigma}(t)d_{\ell\sigma'}(t')> \tag{9}$$

$$G^{>}_{\ell\sigma',\gamma\delta'k'\sigma_1}(t,t') = -\frac{\mathrm{i}}{\hbar}<d_{\ell\sigma'}(t)d^{\dagger}_{\gamma\delta',k'\sigma_1}(t')> \tag{10}$$

The other pair of these kinds of Keldysh Green's functions are defined as:

$$G^{>}_{\gamma\delta'k'\sigma_1,\ell\sigma'}(t',t) = \frac{\mathrm{i}}{\hbar}<d^{\dagger}_{\ell\sigma'}(t)a_{\gamma\delta',k'\sigma_1}(t')> \tag{11}$$

$$G^{>}_{\gamma\delta k\sigma,\ell_1\sigma_1'}(t,t') = -\frac{\mathrm{i}}{\hbar}<a_{\gamma\delta,k\sigma}(t)d^{\dagger}_{\ell_1\sigma_1'}(t')> \tag{12}$$

Up to now, we have defined all of the required Keldysh Green's functions in our system. The time-dependent current function Eq. (4) determined by employing the non-equilibrium Green's functions is

$$\begin{aligned}\Pi_{\gamma\gamma'}(t,t') = -2e^2\mathrm{Re}\sum_{\delta\delta' kk'}\sum_{\ell\ell_1}\sum_{\sigma\sigma'}\sum_{\sigma_1\sigma_1'}\Big\{&\tilde{T}^{\sigma\sigma'}_{\gamma k}(t)\\ &\times\tilde{T}^{\sigma_1\sigma_1'}_{\gamma' k'}(t')G^{<}_{\ell_1\sigma_1',\gamma\delta k\sigma}(t',t)G^{>}_{\ell\sigma',\gamma'\delta'k'\sigma_1}(t,t')\\ &-\tilde{T}^{\sigma\sigma'*}_{\gamma k}(t)\tilde{T}^{\sigma_1\sigma_1'*}_{\gamma' k'}(t')G^{<}_{\gamma'\delta'k'\sigma_1,\gamma\delta k\sigma}(t',t)G^{>}_{\ell\sigma,\ell_1\sigma_1'}(t,t')\\ &-\tilde{T}^{\sigma\sigma'*}_{\gamma k}(t)\tilde{T}^{\sigma_1\sigma_1'}_{\gamma' k'}(t')G^{<}_{\ell_1\sigma_1',\ell\sigma'}(t',t)G^{>}_{\gamma\delta k\sigma',\gamma'\delta'k'\sigma_1}(t,t')\\ &+\tilde{T}^{\sigma\sigma'*}_{\gamma k}(t)\tilde{T}^{\sigma_1\sigma_1'*}_{\gamma' k'}(t')G^{<}_{\gamma'\delta'k'\sigma_1,\ell\sigma'}(t',t)\\ &\times G^{>}_{\gamma\delta k\sigma,\ell_1\sigma_1'}(t,t')\Big\}\end{aligned} \tag{13}$$

Equation (13) contains the information of current-current correlation fluctuations of our system generally. However, the Keldysh Green's functions are intimately related to the concrete system. In order to find these Green's functions we have to solve the Dyson-like equations for these functions.

From the equation of motion method, one obtains the Keldysh Green's function $G^{<}_{\gamma\delta'k'\sigma_1,\gamma\delta k\sigma}(t',t)$ of the terminal:

$$\begin{aligned}G^{<}_{\gamma\delta'k'\sigma_1,\gamma\delta k\sigma}(t',t) &= G^{(0)<}_{\gamma\delta'k'\sigma_1,\gamma\delta k\sigma_1}(t',t)\\ &+\sum_{\ell_1\ell_2}\sum_{\sigma_1'\sigma_2}\int\mathrm{d}t_1\mathrm{d}t_2\,\tilde{T}^{\sigma\sigma_1'*}_{\gamma k}(t_1)\tilde{T}^{\sigma_1\sigma_2}_{\gamma' k'}(t_2)g^{r}_{\gamma\delta',k'\sigma_1}(t',t_2)\\ &\times G^{<}_{\ell_2\sigma_2\ell_1\sigma_1'}(t_2,t_1)g^{a}_{\gamma\delta,k\sigma}(t_1,t)\end{aligned} \tag{14}$$

where $g^{r(a)}_{\gamma\delta,k\sigma}(t_1,t)$ is the retarded (advanced) Green's function of the free electron in the γ th lead, and $G^{(0)}_{\gamma\delta'k'\sigma_1,\gamma\delta k\sigma}(t',t)$ is the Keldysh Green's function of the terminals defined by $G^{(0)<}_{\gamma\delta'k'\sigma_1,\gamma\delta k\sigma}(t',t) = g^{<}_{\gamma\delta,k\sigma}(t',t)\delta_{\gamma\gamma'}\delta_{\delta\delta'}\delta_{kk'}\delta_{\sigma'\sigma_1}$. Correspondingly, the Keldysh Green's function $G^{>}_{\gamma\delta k\sigma,\gamma\delta'k'\sigma_1}(t,t')$ is given by the integral equation associated with the Green's functions of central regime and terminals as:

$$\begin{aligned}G^{>}_{\gamma\delta k\sigma,\gamma\delta'k'\sigma_1}(t,t') &= G^{(0)>}_{\gamma\delta k\sigma,\gamma\delta'k'\sigma_1}(t,t')\\ &+\sum_{\ell_1\ell_2}\sum_{\sigma_1'\sigma_2}\int\mathrm{d}t_1\mathrm{d}t_2\,\tilde{T}^{\sigma\sigma_1'}_{\gamma k}(t_1)\tilde{T}^{\sigma_1\sigma_2*}_{\gamma' k'}(t_2)g^{r}_{\gamma\delta,k\sigma}(t,t_1)\\ &\times G^{>}_{\ell_1\sigma_1',\ell_2\sigma_2}(t_1,t_2)g^{a}_{\gamma'\delta',k'\sigma_1}(t_2,t')\end{aligned} \tag{15}$$

The Keldysh Green's functions related to the correlations between different parts of the system are given by equation of motions and the Langreth relations. The first pair of the Dyson-like equations are expressed by

$$\begin{aligned}G^{<}_{\ell\sigma',\gamma\delta k\sigma}(t',t) = \sum_{\ell_1\sigma_1}\int\mathrm{d}t_1\,\tilde{T}^{\sigma\sigma_1*}_{\gamma k}(t_1)\Big[&G^{r}_{\ell\sigma',\ell_1\sigma_1}(t',t_1)\\ &\times g^{<}_{\gamma\delta,k\sigma}(t_1,t)+G^{<}_{\ell\sigma',\ell_1\sigma_1}(t',t_1)g^{a}_{\gamma\delta,k\sigma}(t_1,t)\Big]\end{aligned} \tag{16}$$

$$\begin{aligned}G^{>}_{\ell\sigma',\gamma\delta'k'\sigma_1}(t,t') = \sum_{\ell_2\sigma_2}\int\mathrm{d}t_1\,\tilde{T}^{\sigma_1\sigma_2*}_{\gamma' k'}(t_1)\Big[&G^{r}_{\ell\sigma',\ell_2\sigma_2}(t,t_1)\\ &\times g^{>}_{\gamma\delta',k'\sigma_1}(t_1,t')+G^{>}_{\ell\sigma',\ell_2\sigma_2}(t,t_1)g^{a}_{\gamma\delta',k'\sigma_1}(t_1,t)\Big]\end{aligned} \tag{17}$$

Correspondingly, we employ the equation of motion method to find the other pair of the Keldysh Green's functions related to the terminals and the central regime as:

$$G^{<}_{\gamma\delta' k'\sigma_1,\ell\sigma'}(t',t)=\sum_{\ell_2\sigma_2}\int \mathrm{d}t_1 \widetilde{T}^{\sigma_1\sigma_2}_{\gamma' k'}(t_1)\Big[g^{r}_{\gamma\delta',k'\sigma_1}(t',t_1) \times G^{<}_{\ell_2\sigma_2,\ell\sigma'}(t_1,t)+g^{<}_{\gamma\delta',k'\sigma_1}(t',t_1)G^{a}_{\ell_2\sigma_2,\ell\sigma'}(t_1,t)\Big] \quad (18)$$

$$G^{>}_{\gamma\delta k\sigma,\ell_1\sigma_1'}(t,t')=\sum_{\ell_2\sigma_2}\int \mathrm{d}t_1 \widetilde{T}^{\sigma\sigma_2}_{\gamma k}(t_1)\Big[g^{r}_{\gamma\delta,k\sigma}(t,t_1) \times G^{>}_{\ell_2\sigma_2,\ell_1\sigma_1'}(t_1,t')+g^{>}_{\gamma\delta,k\sigma}(t,t_1)G^{a}_{\ell_2\sigma_2,\ell_1\sigma_1'}(t_1,t')\Big] \quad (19)$$

Through the equations above, we know that the current correlation functions are determined completely by the Green's functions of the central regime and the terminals together. The interaction effect is also involved in the equations. We have employed the notations for the retarded, advanced, and Keldysh Green's functions in the central regime $G^{X}_{\ell_2\sigma_2,\ell\sigma'}(t_1,t)$, where $X\in\{r,a,<,>\}$.

To proceed with the derivation of the current correlation, we define the following correlation functions in order to express the formulas compactly. The elements of the matrix $\boldsymbol{W}^{<,>}_{\gamma}(t,t')$ is defined by

$$W^{<,>}_{\gamma,\sigma\sigma'}(t,t')=\sum_{\sigma_1}\int \mathrm{d}t_1\Big[G^{r}_{\sigma\sigma_1}(t,t_1)\Sigma^{<,>}_{\gamma,\sigma_1\sigma'}(t_1,t') + G^{<,>}_{\sigma\sigma_1}(t,t_1)\Sigma^{a}_{\gamma,\sigma_1\sigma'}(t_1,t')\Big] \quad (20)$$

The elements of the matrix $\boldsymbol{U}^{<,>}_{\gamma\gamma'}(t,t')$ is defined by

$$U^{<,>}_{\gamma\gamma',\sigma\sigma'}(t,t')=\sum_{\sigma_1\sigma_2}\iint \mathrm{d}t_1\mathrm{d}t_2\Sigma^{r}_{\gamma,\sigma\sigma_1}(t,t_1) \times G^{<,>}_{\sigma_1\sigma_2}(t_1,t_2)\Sigma^{a}_{\gamma',\sigma_2\sigma'}(t_2,t') \quad (21)$$

In the definition above, we used the notation of Green's functions in the central regime as $G^{X}_{\sigma,\sigma'}=\sum_{\ell\ell'}G^{X}_{\ell\sigma,\ell'\sigma'}$. Substituting all of the required functions into the current correlation formula Eq. (13), we find that the interaction strengths and the Green's functions of terminals are combined to form the self-energy functions, which are defined by the relation

$$\Sigma^{X}_{\gamma,\sigma\sigma'}=\sum_{\delta\sigma_1 k}\widetilde{T}^{*}_{\gamma k,\sigma_1\sigma}(t_1)\widetilde{T}_{\gamma k,\sigma_1\sigma'}(t)g^{X}_{\gamma\delta,k\sigma_1}(t_1,t) \quad (22)$$

where $X\in\{r,a,<,>\}$. By employing the relations between the non-equilibrium Green's functions as

$$G^{<}_{\sigma\sigma'}(t,t')^{*}=-G^{>}_{\sigma'\sigma}(t',t) \quad (23)$$

$$G^{a}_{\sigma\sigma'}(t,t')^{*}=G^{r}_{\sigma'\sigma}(t',t) \quad (24)$$

and the relations between the self-energies as

$$\Sigma^{<}_{\gamma,\sigma\sigma'}(t,t')^{*}=-\Sigma^{>}_{\gamma,\sigma'\sigma}(t',t) \quad (25)$$

$$\Sigma^{a}_{\gamma,\sigma\sigma'}(t,t')^{*}=\Sigma^{r}_{\gamma,\sigma'\sigma}(t',t) \quad (26)$$

half of the terms in Eq. (13) can be attributed to the imaginary parts of the other. Therefore from Eq. (13) and the related formulas, we immediately find the current correlation function by the matrix form

$$\Pi_{\gamma\gamma'}(t,t')=-4e^{2}\mathrm{Re}\Big\{\mathrm{Tr}\Big[\boldsymbol{W}^{<}_{\gamma}(t',t)\boldsymbol{W}^{>}_{\gamma'}(t,t') -\delta_{\gamma\gamma'}\boldsymbol{\Sigma}^{<}_{\gamma}(t',t)\boldsymbol{G}^{>}(t,t')-\boldsymbol{U}^{<}_{\gamma'\gamma}(t',t)\boldsymbol{G}^{>}(t,t')\Big]\Big\} \quad (27)$$

The notation "Tr" represents the procedure by taking trance over the spin space of the matrices. The matrix $\boldsymbol{G}^{X}(t,t')$ where $X\in\{r,a,<,>\}$, indicates the Green's function matrix of the central regime with the elements $G^{X}_{\sigma\sigma'}(t,t')$. This is the more general result of the current-current fluctuation correlation function, which is associated with the concrete structures of the central regime and terminals. The perturbation information due to the external fields is also involved in the formula. When the system is a spin-degenerate one, the matrices above become ordinary functions, and the notation for trace "Tr" has no contribution to the formula. The spectral density of noise is determined by taking a Fourier transformation over two times to give the quasi-equilibrium function $S_{\gamma\gamma'}(\Omega)$ satisfying the relation:

$$S_{\gamma\gamma'}(\Omega)\delta(\Omega+\Omega')=\frac{1}{2\pi}\Pi_{\gamma\gamma'}(\Omega,\Omega') \quad (28)$$

Therefore, by making a Fourier transformation over Eq. (27) we can obtain the spectral density of noise. Here we present the Fourier transformation of current correlation with respect to Ω and Ω' as the following relation:

$$\Pi_{\gamma\gamma'}(\Omega,\Omega')=-\left(\frac{2e}{h}\right)^{2}\mathrm{Re}\int d\varepsilon d\varepsilon'\mathrm{Tr}\Big\{\boldsymbol{W}^{<}_{\gamma}(\varepsilon'+\hbar\Omega',\varepsilon) \times\boldsymbol{W}^{>}_{\gamma'}(\varepsilon+\hbar\Omega,\varepsilon')-\boldsymbol{U}^{<}_{\gamma'\gamma}(\varepsilon'+\hbar\Omega',\varepsilon)\boldsymbol{G}^{>}(\varepsilon+\hbar\Omega,\varepsilon') -\delta_{\gamma\gamma'}\Sigma^{>}_{\gamma}(\varepsilon'+\hbar\Omega',\varepsilon)\boldsymbol{G}^{>}(\varepsilon+\hbar\Omega,\varepsilon')\Big\} \quad (29)$$

In the above formula, the Fourier transformation of the matrix $\boldsymbol{W}^{<,>}_{\gamma}(\varepsilon,\varepsilon')$ is determined by

$$\boldsymbol{W}^{<,>}_{\gamma}(\varepsilon,\varepsilon')=\frac{1}{2\pi\hbar}\int \mathrm{d}\varepsilon_1[\boldsymbol{G}^{r}(\varepsilon,\varepsilon_1)\boldsymbol{\Sigma}^{<,>}_{\gamma}(\varepsilon_1,\varepsilon') + \boldsymbol{G}^{<,>}(\varepsilon,\varepsilon_1)\boldsymbol{\Sigma}^{a}_{\gamma}(\varepsilon_1,\varepsilon') \quad (30)$$

The Fourier transformation of the matrix $\boldsymbol{U}^{<,>}_{\gamma'\gamma}(\varepsilon,\varepsilon')$ in the Fourier transformed current correlation function is determined by

$$\boldsymbol{U}^{<,>}_{\gamma'\gamma}(\varepsilon,\varepsilon')=\left(\frac{1}{2\pi\hbar}\right)^{2}\iint \mathrm{d}\varepsilon_1\mathrm{d}\varepsilon_2\Sigma^{r}_{\gamma'}(\varepsilon,\varepsilon_1) \times\boldsymbol{G}^{<,>}(\varepsilon_1,\varepsilon_2)\boldsymbol{\Sigma}^{a}_{\gamma}(\varepsilon_2,\varepsilon') \quad (31)$$

Since the Green's functions of the central regime and terminals are related to concrete systems, they can be derived once the Hamiltonians of the systems are given. Therefore, we can find the spectral density of current noise from Eq. (29) for a specific system. The effect of the external ac fields is contained in the self-energy of the terminals, and it is also involved in the Green's functions of the central regime. Thermal noise and shot noise are included in Eq. (29) since

temperature is non-zero. When temperature approaches zero, thermal noise disappears, and the excess noise is shot noise.

3 Toroidal carbon nanotube systems

The toroidal carbon nanotube (TCN) is a form of torus carbon structure created by bending the carbon tube such that the two edges are connected [25–28]. The TCN is formed by rolling a finite graphite sheet from the origin to the vectors $\boldsymbol{R}_x = m_1\boldsymbol{a}_1 + m_2\boldsymbol{a}_2$, and $\boldsymbol{R}_y = p_1\boldsymbol{a}_1 + p_2\boldsymbol{a}_2$ simultaneously. It is denoted by $(m_1, m_2; p_1, p_2)$ as convention, and it satisfies the periodic boundary conditions along both of the longitudinal and transverse directions. Two kinds of TCN with highly symmetric structures are armchair $(m, m; -p, p)$ TCN and zigzag $(m, 0; -p, 2p)$ TCN. This kind of carbon material has specific electronic structure, and it can be used to make the interference devices. Compared with a normal metal or semiconductor ring, TCN can carry a larger persistent current due to the modification of the energy structure and energy gap. Recently, research on electron transport through device structure has been presented for the new stage of investigation in which the carbon devices are coupled to different materials. The material structure and electronic properties of terminals are involved in the output characteristics of the system. The Aharonov-Bohm effect presents very important contribution to the mesoscopic transport due to the modification of the energy gap of TCN. We have investigated the mesoscopic transport through the systems with a TCN coupled to a normal metallic and a superconducting leads (N-TCN-S), the dc Josephson current through a TCN coupled to superconducting leads (S-TCN-S), and the system with a quantum dot embedded in one arm of the TCN [29–31]. We have also investigated the system under the application of microwave fields, and the photon-assisted tunneling was deemed to be associated with the structure of the system intimately [32, 33]. Here we consider the current noise in the TCN system coupled to normal metal leads, where external microwave fields irradiate to the terminals. The system is composed of three parts: the central TCN, and the normal metal leads. The central TCN is applied with a static magnetic field $\boldsymbol{B}$ perpendicular to the ring, which induces a magnetic flux ϕ threaded through the TCN [34, 35]. The electrons are free from the magnetic field $\boldsymbol{B}$, but the vector potential $\boldsymbol{A}$ affects the behaviors of electrons due to the Aharonov-Bohm effect. The electrons of the leads are described by the grand canonical ensembles, and the central TCN is described by the tight-binding Hamiltonian. We consider the circumstance that the two leads are biased by the dc voltage V, which is the drop of chemical potentials of the two leads $\mu_L - \mu_R = eV$. The microwave field with frequency ω is applied to the γth lead forming potential drop $e\tilde{V}_{\gamma d}\cos(\omega t)$ in it. The symmetric system is studied by setting $\Gamma = 2\Gamma_L = 2\Gamma_R$, and $\lambda_L = \lambda_R = \lambda$. We perform the numerical calculations at zero temperature. The photon energy of the fields is scaled by the parameter γ_0 as $\hbar\omega = 0.01\,\gamma_0$. We only display the special case for $S_{LL}(0) = S$ as an example here.

We present the oscillation behaviors for the differential shot noise versus magnetic flux in Fig. 2 to show detailed oscillation structures. We only depict the behaviors of type I (7,7; −75,75) and type II (7,7; −74,74) TCN systems for illustration purpose. The periodic oscillation structures are also exhibited, however, the period of the structures is $3\phi_0$ instead of ϕ_0. This is not the period of single resonant peak oscillation, but is the period of a cluster resonant oscillation. Different TCN systems present different oscillations of $\mathrm{d}S/\mathrm{d}V$. The symmetric property $\mathrm{d}S(\phi)/\mathrm{d}V = \mathrm{d}S(-\phi)/\mathrm{d}V$ is satisfied as shown in this figure.

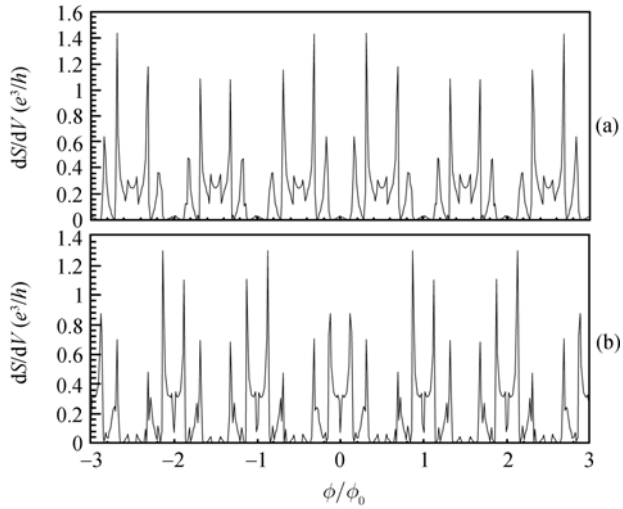

Fig. 2 The differential shot noise $\mathrm{d}S/\mathrm{d}V$ versus magnetic flux ϕ for balanced absorption. The parameters are chosen as $\lambda = 0.8$, $eV = 0.2\gamma_0$. Diagram **(a)** is associated with (7,7; −74,74), and diagram **(b)** is for (7,7; −75,75), correspondingly.

We depict the differential shot noise versus source-drain bias eV in Fig. 3 to study the resonant behavior of shot noise. Different values of $\mathrm{d}S/\mathrm{d}V$ are shown in the diagrams for different TCN systems, and detailed resonant behaviors are seen to associate with the microwave fields as well. Each of the resonant peaks corresponds to a step of the shot noise, and one observes that resonant structure intimately relies on the detailed mesoscopic structure. When $eV < 0$ the differential shot noise is negative while for $eV > 0$ it is positive. This indicates that the shot noise declines to zero as eV increases to zero from the negative regime, while the shot noise increases as eV increases from zero to a definite positive value. We make the comparison of differential shot noise for the same type II (7,7; −74,74) TCN system by considering $\lambda = 0$, and 0.8 shown in Fig. 3 (a) and (b). Some of the resonant peaks are suppressed, while some of them are enhanced due to the applied fields. The resonant peaks in the regime $|eV| < 0.44\gamma_0$ are much smaller than those in the regime $|eV| > 0.44\gamma_0$. Figure 3 (c) and (d) show different behaviors

of dS/dV for the type I (7,7; −75,75) and type III (7,0; −75,150) TCNs. Comparing with Fig. 3 (a), one can observe that the resonant structures are quite different, which are strongly associated with the detailed nano-structure of our system.

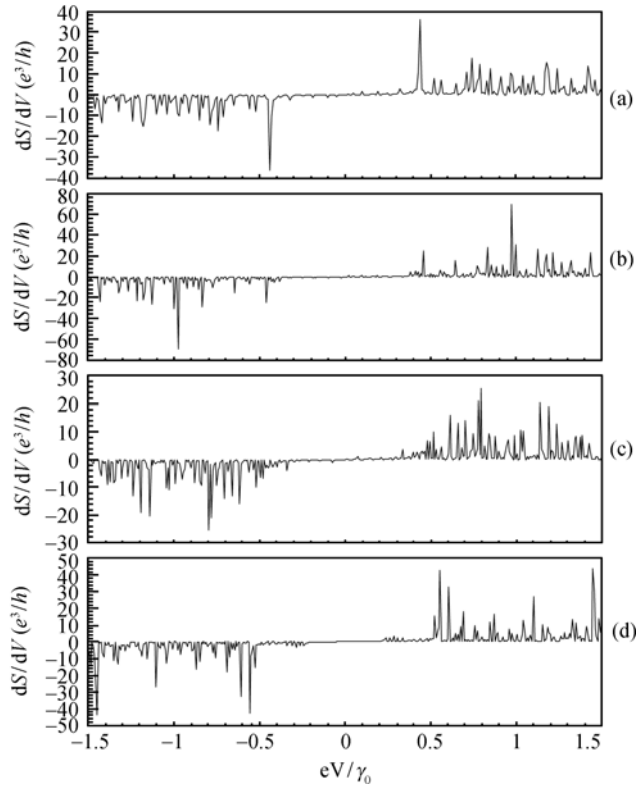

Fig. 3 The differential shot noise dS/dV versus source-drain bias eV as ϕ = 0 for balanced absorption. Diagrams **(a)** and **(b)** correspond to the cases as (7,7; −74,74) for λ = 0.8 and λ = 0. Diagrams **(c)** and **(d)** are associated with λ = 0.8 for (7,7; −75,75) and (7,0; −75,150).

Figure 4 shows the oscillation behaviors of the shot noise with respect to the magnetic flux ϕ. It is obviously seen that the oscillation structure is intimately associated with the concrete structure of the TCN system, and different TCN systems show different oscillation behaviors. However, the oscillation period is ϕ_0 for all of the different TCN systems. For the type II (7,7; −160,160) TCN system, the oscillation structure is depicted in Fig. 4 (a), from which one observes that a small oscillation is embedded in the valleys of the large oscillation forming compound structure. For the type I (7,7; −75,75) and type II (7,7; −74,74) TCN systems, we find that the oscillations possess a phase difference $\phi_0/2$. The application of microwave fields shifts the magnitude of the shot noise, which is exhibited in Fig. 4 (b). The symmetry property $S(\phi) = S(-\phi)$ is satisfied as shown from the oscillation structures.

The oscillation behaviors of Fano factor with respect to the magnetic flux ϕ are depicted in Fig. 5 for different systems as $eV = 0.3\gamma_0$ and $\lambda = 0.5$. The periodic structures of the Fano factor are shown in the period ϕ_0. The magnitudes of the Fano factor is around 0.4, and different TCN systems show different oscillation configurations. The oscillation structures are determined by the shot noise and tunneling current versus ϕ together. These oscillation structures indicate that the shot noise and tunneling current behave differently with respect to the magnetic flux. From the figures above, we conclude that the shot noises of our balanced system are sub-Poissonian. The suppression of shot noise is intimately dependent on the concrete construction of each TCN system, as well as on the applied fields.

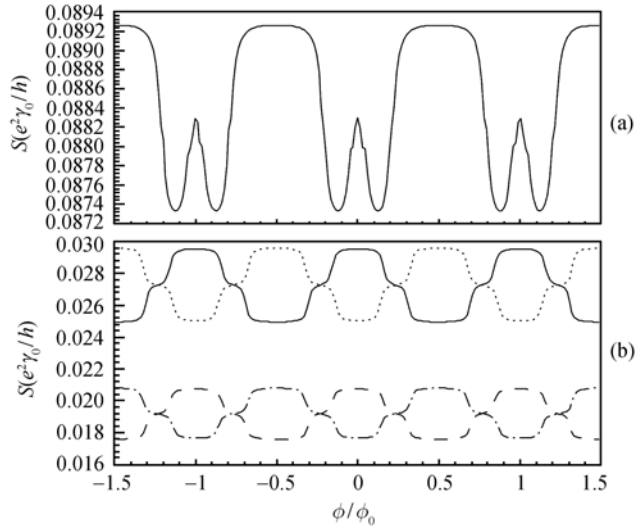

Fig. 4 The shot noise S versus magnetic flux ϕ for balanced absorption. Diagram **(a)** is related to (7,7; −160, 160) as λ = 0.5, and $eV = 0.3\gamma_0$. In diagrams **(b)** the parameter $eV = 0.2\gamma_0$, and the solid, dashed curves are related to (7,7; −74,74) as λ = 0.5, and λ = 0.8, respectively; the dotted, dash-dotted curves correspond to (7,7; −75,75) as λ = 0.5, and λ = 0.8, respectively.

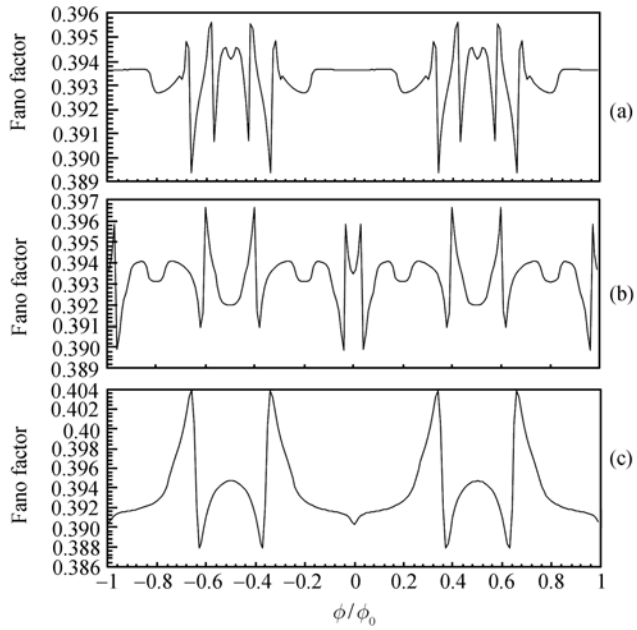

Fig. 5 The Fano factor versus magnetic flux ϕ as λ = 0.5, $eV = 0.3\gamma_0$ for balanced absorption. Diagrams **(a)**, **(b)**, and **(c)** correspond to (7,7; −74,74), (7,7; −75,75), and (7,0; −75,150), respectively.

We present the differential shot noise versus photon energy $\hbar\omega$ as $\Gamma = 0.001\gamma_0$ in Fig. 6 to show the resonant structures for different types of TCN in the absence of-source-drain bias $V = 0$. There exist no resonant peaks as $\hbar\omega < 0.15\gamma_0$ for the type III (7,0; −75,150) TCN asdepicted in Fig. 6 (a). As the photon energy $\hbar\omega > 0.15\gamma_0$ resonant peaks appear with different heights. Compared with the type III TCN, Fig. 6 (b) displays the resonant structure for the type I (7,7; −75,75) TCN, which appears quite differently from the type III TCN. We also observe that there exist no resonant peaks in the regime $\hbar\omega < 0.08\gamma_0$. The resonant structures are intimately related to the concrete of TCNs, as well as the ac fields. In some regimes the resonant peaks are enhanced for one kind of TCN, while for the other kind of TCN they may be suppressed. The positions of resonant peaks are associated with the hybrid energy levels, which are dispersion curves of TCN incorporated with the side-bands of ac fields. The magnitudes of the peaks are dependent on the detailed nature of TCN, and they are modified by the Bessel functions associated with the applied fields.

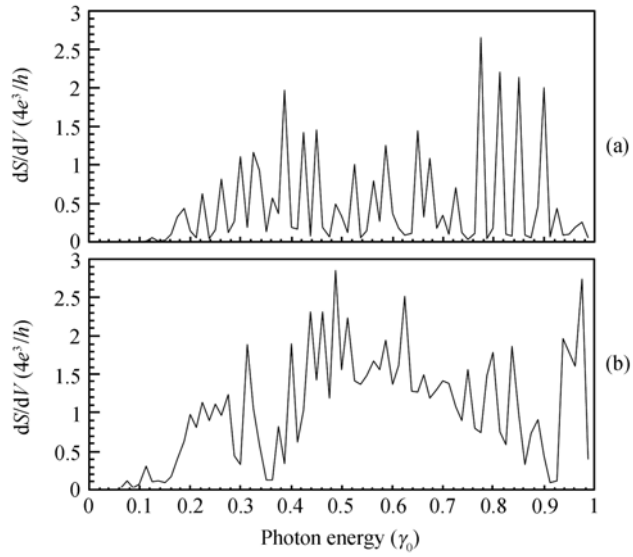

Fig. 6 The differential shot noise dS/dV of the unbalanced absorption case versus photon energy $\hbar\omega$ at zero temperature as $eV = 0$. The parameters are chosen as $\phi = 0$, $e\tilde{V}_{\gamma d} = 0.8\gamma_0$, and $\Gamma = 0.001\gamma_0$. Diagrams **(a)** and **(b)** correspond to the (7,0; −75,150) and (7,7; −75,75) TCNs, respectively.

4 Concluding remarks

The more general current correlation and shot noise formulas are derived by employing the non-equilibrium Green's function technique in the presence of external ac fields. The noise is determined by the concrete structures of our mesoscopic systems and the applied ac fields. The main formula is given by Eqs.(27) and (29), which are valid for the system with the central regime being a mesoscopic sample including electron-electron interaction. The central regime can be a quantum dot and the finite carbon nanotubes. On the other hand, the terminals can be made of metallic, ferromagnetic leads. The detailed structure of each part plays an important role in the current noise. We have made the numerical calculations on the system with a toroidal carbon nanotube coupled to two normal metallic leads, and the microwave fields induce novel behaviors for the current noise. The sub-Poissonian and super-Poissonian noise may exist in the same system. The concrete forms of external fields are important in the noise, and the side-bands of fields provide additional channels for electron to tunnel. Therefore, the correlations of transporting electrons may exist in the same channels of intrinsic nano-devices, as well as between different channels among the intrinsic channels and side-bands of external fields. This effect induces novel shot noise in our mesoscopic systems.

Acknowledgements This work was supported by the National Natural Science Foundation of China (Grant No. 10375007).

References

1. van der Ziel A., Noise in Solid State Devices and Circuits, New York: Wiley, 1986
2. Davenport W. B. and Root W. L., An Introduction to the Theory of Random Signals and Noise, New York: IEEE Press, 1987
3. Callen H. B. and Welton T. W., Phys. Rev., 1951, 83: 34–40
4. Nyquist H., Phys. Rev., 1928, 32: 110–113
5. Blanter Ya. M. and Büttiker M., Phys. Rep., 2000, 336: 1–166
6. de Jong M. J. M. and Beenakker C. W. J., Phys. Rev. B, 1992, 46: 13400–13406
7. de Jong M. J. M. and Büttiker M., ibid., 1994, 49: 16070–16073
8. Yurke B. and Kochanski G. P., Phys. Rev. B, 1990, 41: 8184–8194
9. Beenakker C. W. J. and van Houten H., Phys. Rev. B, 1991, 43: 12066–12069
10. Büttiker M., Phys. Rev. Lett., 1992, 68: 843–846
11. Büttiker M., Phys. Rev. B, 1992, 46: 12485–12507
12. Davies J. H., Hyldgaard P., Hershfield S., and Wilkins J.W., Phys. Rev. B, 1992, 46: 9620–9633
13. Hanke U., Galperin Y. M., Chao K. A., and Zou N., Phys. Rev. B, 1993, 48: 17209–17216
14. Sun Q. F., Wang J., and Lin T. H., Phys. Rev. B, 2000, 61: 13032–13036
15. Aguado R. and Kouwenhoven L. P., Phys. Rev. Lett., 2000, 84: 1986–1989
16. Zhao H. K., Phys. Rev. B, 2001, 63: 205327–205331
17. Li Y. P., Zaslavsky A., Tsui D. C., Santos M., and Shayegan M., Phys. Rev. B, 1990, 41: 8388–8391
18. Henny M., Oberholzer S., Strunk C., and Schönenberger C., Phys. Rev. B, 1999, 59: 2871–2880
19. Korotkov A. N. and Likharev K. K., Phys. Rev. B, 2000, 61, 15975–15987
20. Iannaccone G., Lombardi G., Macucci M., and Pellegrini B., Phys.

Rev. Lett., 1998, 80: 1054–1057
21. Kuznetsov V. V., Mendez E. E., Bruno J.D., and Pham J. T., Phys. Rev. B, 1998, 58: R10159–R10162
22. Blanter Y. M. and Büttiker M., Phys. Rev. B, 1999, 59: 10217–10226
23. Schiller A. and Hershfield S., Phys. Rev. B, 1998, 58, 14978–15010
24. Lesovik G. B. and Levitov L. S., Phys. Rev. Lett., 1994, 72: 538–541
25. Dunlap B. I., Phys. Rev. B, 1992, 46: 1933–1936
26. Itoh S., Ihara S., and Kitakami J., Phys. Rev. B, 1993, 47: 1703–1704
27. Haddon R. C., Nature (London), 1997, 388: 31–40
28. Lin M. F. and Chuu D. S., Phys. Rev. B, 1998, 57: 6731–6737
29. Zhao H. K., Phys. Lett. A, 2003, 310: 207–213
30. Zhao H. K., Phys. Lett. A, 2003, 308: 226–233
31. Zhao H. K., Phys. Lett. A, 2003, 317: 329–335
32. Zhao H. K. Eur. Phys. J. B, 2003, 33: 365–372
33. Zhao H. K. and Wang J., Eur. Phys. J. B, 2004, 40: 93–100
34. Zhao H. K. and Wang J., Phys. Lett. A, 2004, 325: 407–414
35. Zhao H. K. and Wang J., to be published in Phys. Rev. B, 2006